

# CORNER: A Step Towards Realistic Simulations for VANET

Eugenio Giordano \*  
University of California Los Angeles  
Computer Science Department  
Los Angeles, California  
giordano@cs.ucla.edu

Raphael Frank  
University of Luxembourg  
Department of Computer Science  
Luxembourg  
raphael.frank@uni.lu

Giovanni Pau  
University of California Los Angeles  
Computer Science Department  
Los Angeles, California  
gpau@cs.ucla.edu

Mario Gerla  
University of California Los Angeles  
Computer Science Department  
Los Angeles, California  
gerla@cs.ucla.edu

## ABSTRACT

Advances in portable technologies and emergence of new applications stimulate interest in urban vehicular communications for commercial, military, and homeland defense applications. Simulation is an essential tool to study the behavior and evaluate the performance of protocols and applications in large-scale urban vehicular networks.

In this paper we propose CORNER a low computational cost yet accurate urban propagation model for mobile networks. CORNER estimates the presence of buildings and obstacles along the signal path using information extrapolated from urban digital maps. A reverse geocoding algorithm is used to classify the propagation situation of any two nodes that need to communicate starting from their geographical coordinates. Sender and Receiver are classified as in Line of Sight if there are no obstacles in between, and as NON in Line of Sight when there are obstacles (i.e. buildings) between them. CORNER has been validated through extensive on-the-road experiments, the results show high accuracy in predicting the network connectivity. In addition, on-the-road experiments suggest the need to refine the fading model to differentiate between Line of Sight, and NON Line of Sight situations. Finally, we show the impact of CORNER on simulation results for widely used applications.

---

\*Eugenio Giordano is also affiliated with University of Bologna, DEIS, WiLab, Bologna, Italia

Permission to make digital or hard copies of all or part of this work for personal or classroom use is granted without fee provided that copies are not made or distributed for profit or commercial advantage and that copies bear this notice and the full citation on the first page. To copy otherwise, to republish, to post on servers or to redistribute to lists, requires prior specific permission and/or a fee.

VANET'10, September 24, 2010, Chicago, Illinois, USA.  
Copyright 2010 ACM 978-1-4503-0145-9/10/09 ...\$10.00.

## Categories and Subject Descriptors

C.2.1 [Computer Systems Organization]: Computer-Communication Networks—*Wireless Communication*

## General Terms

Design

## Keywords

VANET, Urban Propagation, Model.

## 1. INTRODUCTION

Vehicular Ad Hoc Networks (VANETs) are the first practical step towards the deployment of urban ad hoc networks. WiFi enabled smart devices will provide the first platform for a field deployment of vehicular applications and protocols. As standards are established, OEM based WiFi deployments will be replaced by Dynamic Short Range Communication (DSRC) radios that comply with the upcoming *IEEE802.11p* standard [1].

In city scenarios, characterized by thousands of cars, non uniform density and irregular propagation obstacles [2] [3], it is imperative to study scalability and performance of the applications and protocols that run on such scenarios. Obviously, the prohibitive costs (and the privacy implications) of real field experiments with thousands of instrumented vehicles forces researchers and developers to fall back to simulation models and tools, augmented with the results from limited actual experiments. Simulation fidelity is particularly important to get realistic results. In particular, propagation and mobility fidelity are key to evaluate the performance of vehicular network protocols and applications in urban scenarios. However, to this day, to the best of our knowledge, there is very limited access to computationally efficient urban propagation models.

Urban scenarios are characterized by buildings that constitute an obstruction to the free space radio waves propagation. In order to perform high-fidelity simulations, with a more realistic propagation, buildings simply cannot be ignored. In principle, it would be

possible to compute the path loss very accurately using Ray Tracing or similar techniques [4]. However, these techniques require a very detailed information about the environment to simulate, such as a tridimensional description of the environment or the reflection index of all the surfaces in the environment [5]. Gathering information on buildings material, shape, and reflection index is a difficult task that requires the allocation of specific resources for each building. For instance the blueprints of the buildings need to be inspected and the reflection index of each construction material needs to be experimentally studied or otherwise assessed. Thus resulting in almost impossible task especially for large urban areas. Furthermore these techniques have a very high computational cost often resulting in several months of CPU cycles. Therefore, due to resource and time constraints, most of the current literature, based on simulation studies, assumed a *flat* propagation model (e.g. the “Two Ray” model) that computes a deterministic component of the Path Loss based on the geometric distance between two nodes. In this case, obstructions are represented statistically, introducing a probabilistic component called shadowing. The shadowing is an additional Path Loss, usually log-normally distributed, that emulates the movement of the nodes around large obstacles such as buildings. This probabilistic component, however, can not be related to the environment the nodes are moving in, i.e. the urban street grid, voiding all efforts in accurately representing vehicular mobility.

In the current literature there exist several path loss prediction formulae that are suitable for urban environment and that are not computationally expensive. However these formulae cannot be directly implemented for network simulators. In fact these formulae require information about the relative position of nodes with regards to the surrounding environment. In this paper we present CORNER, a novel path loss prediction scheme, that extrapolates this information from the road map, allowing the application canonical path loss prediction formulae in network simulators. CORNER represents a good trade-off between accuracy of prediction the Path Loss and computational complexity. In addition, CORNER deterministically accounts for obstructions relatively to the environment the vehicles are moving in, enhancing the benefit of better representing the vehicular mobility.

The remainder of this paper is organized as follows: in Section 2 we describe the model in detail; in Section 3 we present the results of our experimental validation campaign; in Section 4 we show the impact that a better propagation model has on simulation results; in Section 5 we present the related work and finally in Section 6 we conclude our paper.

## 2. CORNER DESCRIPTION

### 2.1 Overview

Most of the existing path loss prediction formulae are specifically devised for path loss calculation between a base station and a mobile. They address very different types of obstacles than those impacting Vehicle-to-Vehicle (V2V) communications (see Section 5). CORNER uses the path loss prediction formulae presented in [6]. Those formulae deterministically account for obstructions on the signal path between vehicles and assume both transmitter and receiver antennas are set at low heights (1.5 meters). The formulae cannot be applied without the knowledge of the surrounding environment and of the geometric properties of the signal path (e.g. distance between transmitter and crossroads). CORNER extracts (and extrapolates) this information from the road topology map, allowing the application of the formulae in simulation. The path loss prediction procedure can be summarized in three subsequent steps:

- **Reverse Geocoding:** given a pair of nodes, map each node onto a road segment. The shortest road path between these two road segments represents the path that the signal will traverse.
- **Propagation Situation Classification:** use the geometrical properties of the road network to assess if the two nodes are in line of sight or behind a corner.
- **Formulae Application:** compute all geometrical distances involved in the application of the Path Loss prediction formula.

In the following we will discuss in detail each of these steps.

### 2.2 Reverse Geocoding

Reverse Geocoding procedures are used to map a given geographical position onto the road topology. These techniques are commonly used by commercial navigation systems to correct the positioning error of the GPS receivers. Conventional techniques usually represent road segments as one-dimensional lines. Each position is then mapped on the geometrically closest segment. Taking advantage of available space/time correlation, unsuitable mappings are filtered out, removing spikes from position estimates. However these techniques can not be applied in this case, if not to filter out positioning errors. Indeed, the purpose of the reverse geocoding performed by CORNER is not to estimate on which road segment each single node is traveling, but to assess what are the obstructions present on the signal propagation path between pairs of nodes. As we will see in the next section, the road segments are used to build a geometrical model of the environment, it is then more important to select the actual road segments the signal will traverse and not the ones the vehicles are actually traveling on. For this purpose we assign to each road segment a *proximity area*. This proximity area is defined as the surface that includes all locations that are at a distance smaller than  $RW/2$  from the road segment. A graphical representation of the proximity area is shown in Figure 1(a).  $RW$  is the road segment width and it is computed as follows:

$$RW = (NoL * LW) + 10 \quad (1)$$

Where  $NoL$  is the number of lanes and the units are expressed in meters (N.B. the number of lanes is double if the segment is part of a two way road).  $LW$  represents the lane width, that we assume constant. In addition we consider the roads 10 meters larger to take into account the sidewalk. Each node is assigned a set of candidate road segments. The candidates are all the road segments of which a node is in the proximity area. Consider a pair of nodes. We must identify the propagation path and estimate the loss between the pair. To identify the path, among the sets of road segments associated with the pair, CORNER selects the two segments (one for each node) that involve the least number of intersections to traverse. Let us consider the example represented in Figure 1(b). For vehicle A there will only be a single candidate road segment (segment number 1). For vehicle B instead all the four segments are candidates. The best connected pair of segments is segment 1 itself, therefore vehicles A and B will be mapped onto the same segment. It is important to notice that traditional reverse geocoding techniques, that map vehicles onto the road segment closest to them, would have mapped node B onto segment number 2. If a pair of nodes cannot be mapped on two segments connected at most through two intersections, the nodes are considered to be too far away from each other and the Path Loss between them is set to a fixed threshold. This threshold is high enough so that the network simulator will not consider this pair of nodes as neighbors. The

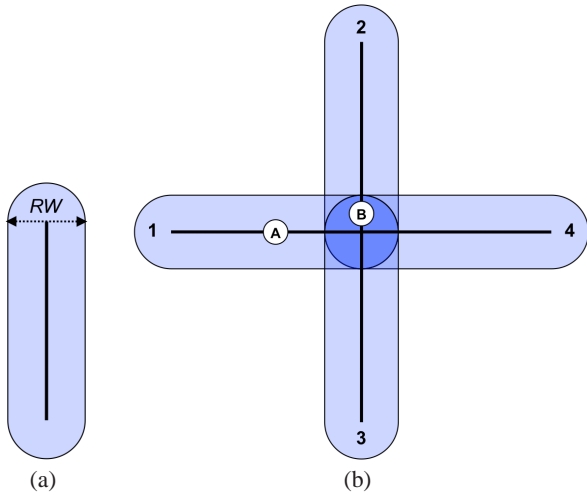


**Figure 1: (a) Single road segment proximity area; (b) Example of different candidates sets for Reverse Geocoding**

Overtraversed intersections generated by the Reverse Geocoding are used in the Propagation Situation Classification described in the next paragraph.

### 2.3 Propagation Situation Classification

Namely, the Path Loss (PL) is a function of the relative position of two nodes. CORNER classifies each pair of vehicles into three possible cases: Line Of Sight (LOS), Non Line Of Sight with one corner along the path (NLOS1) and Non Line Of Sight with two corners along the path (NLOS2). This classification leverages the result of Reverse Geocoding using road segments and crossroads that interconnect them. In order to perform this classification we need to introduce the concept of *angular view* of a node. The angular view of a vehicle is the portion of plane that the vehicle can see from the opening offered by the crossroad. A graphical representation is shown in Figure 2. The opening offered by the crossroad depends on the footprint of the buildings surrounding it. The building footprints for an entire city, although public, are very hard to obtain, as there is no digital database yet. For this reason we consider as building everything that is not a road. Roads are considered as open space where the signal can propagate freely. The road width is defined in equation 1. Each node pair is then classified as follows:

**LOS.** Two vehicles are considered in line of sight if they are mapped on the same road segment. They are also considered in line of sight if they are mapped on two road segments connected by a crossroad and one of them is in the angular view of the other. In addition, two vehicles could be in line of sight if they are mapped on two road segments separated by two crossroads. In this case one of the considered vehicles has two different angular views, one per crossroad. Let us define the two angular views as  $AW_A$  and  $AW_B$  generated respectively by the closest and farthest crossroads. If the other vehicle is traveling inside  $AW_B$  and  $AW_B$  is fully contained inside  $AW_A$  then the two vehicles are in line of sight. A graphical explanation for the latter situation is shown in Figure 3.

**NLOS1.** Two vehicles are considered in NLOS1 if they are mapped on two adjacent road segments and they are not in the angular view of each other, as shown in Figure 2. Two vehicles are also consid-

ered in NLOS1 if they are mapped on two road segments that are separated by two crossroads and one of the vehicles is in LOS with the farthest crossroad, as shown in Figure 3.

**NLOS2.** Two vehicles are considered in NLOS2 if they are mapped on two road segments separated by two crossroads and are nor in LOS or NLOS1, as shown in Figure 3.

Each pair of nodes that passed the first reverse geocoding screening will be classified in one of these situations. This classification is then used to apply the relative path loss prediction formula.

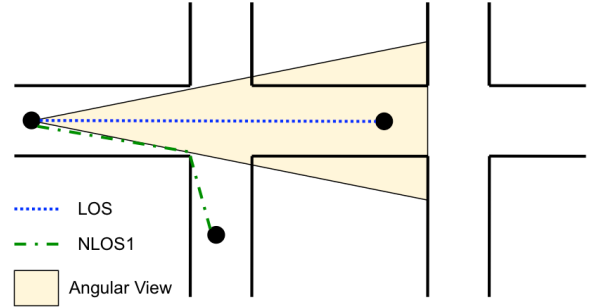


**Figure 2: Propagation: Graphical example for vehicles mapped on adjacent road segments**

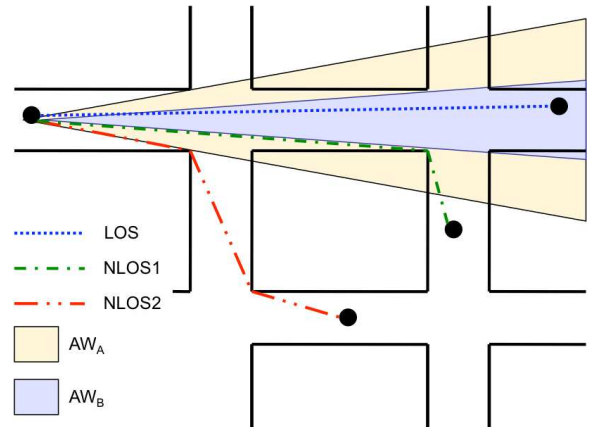


**Figure 3: Propagation: Graphical example for vehicles mapped on road segments separated by 2 crossroads**

### 2.4 Formulae Application

After the classification of the propagation situation has been performed, some more geometric computations are needed in order to apply the formulae. CORNER provides the deterministic component of the path loss due to the surrounding buildings. In order to account for reflections and diffractions from smaller and less predictable objects such as other vehicles or trees, an additional fast fading component should be taken into account. In the following we present the geometric distances that need to be calculated in order to compute the path loss (PL) in each of the three possible situations:

**LOS.**

If the two vehicles are in line of sight the dominant component of the Electro-Magnetic Field (EMF) will be relative to the direct path to the destination. For this reason the simple free space

attenuation formula can be applied:

$$PL = 20 \log \left( \frac{\lambda}{4\pi d} \right) \quad (2)$$

where  $\lambda$  is the wavelength and  $d$  is the distance between the two vehicles.

### NLOS1.

If the two vehicles are not in line of sight with one corner along the path, there is no dominant component for the *EMF*. Therefore the received power will be the sum of the powers of all the rays that are either reflected or diffracted by the surrounding buildings. Figure 4 shows an example situation of two vehicles in NLOS1.

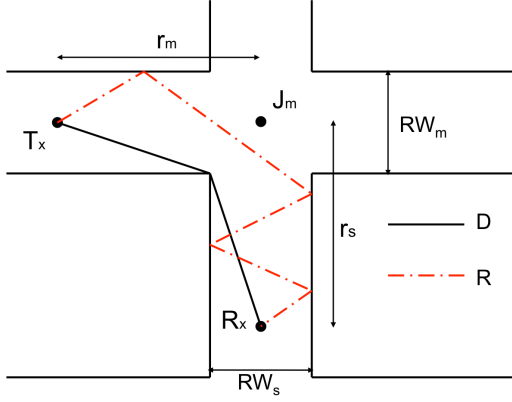


**Figure 4: Graphical example of the geometry in the case NLOS1**

With respect to Figure 4,  $T_x$  and  $R_x$  represent respectively transmitter and receiver,  $J_m$  represents the central point of the intersection of the two road segments on which transmitter and receiver are mapped.  $r_m$  is the distance between  $T_x$  and  $J_m$  and  $r_s$  is the distance between  $J_m$  and  $R_x$ . The total *PL* towards  $R_x$  can be decomposed into two main components:  $PL_R$  which is the path loss encountered by all rays reflected on the surrounding buildings (red dashed path in Figure 4), and  $PL_D$  which is the path loss encountered by the rays diffracted on the corner at the intersection (black solid path in Figure 4). If  $R_x$  is closer to  $J_m$  than  $T_x$  ( $r_s < r_m$ ) then  $PL_R$  is the dominant component, otherwise  $PL_D$  will be the dominant component.  $PL_R$  and  $PL_D$  are functions of the wavelength,  $r_m$ ,  $r_s$  and the road widths  $RW_m$  and  $RW_s$  computed as shown in Equation 1. We refer to the original paper [6] for further details on how to compute these components. Finally the total *PL* is then equal to the sum of these two components:

$$PL = 10 \log \left( 10^{\frac{PL_D}{10}} + 10^{\frac{PL_R}{10}} \right) \quad (3)$$

### NLOS2.

Figure 5 shows an example situation of two vehicles ( $T_x$  and  $R_x$ ) that are not in Line of Sight with two corners along the signal path (NLOS2). Similarly to the NLOS1 case we define the center of the first intersection along the path as  $J_m$  and the centre of the second intersection along the path as  $J_p$ . We then define the distance between  $T_x$  and  $J_m$  as  $r_m$ , the distance between  $J_m$  and  $J_p$  as  $r_s$  and the distance between  $J_p$  and  $R_x$  as  $r_p$ . In addition  $RW_m$  is the width of the road which  $T_x$  is mapped on,  $RW_s$  is the width of the road between  $J_m$  and  $J_p$  and  $RW_p$  is the width of the road  $R_x$  is mapped on.

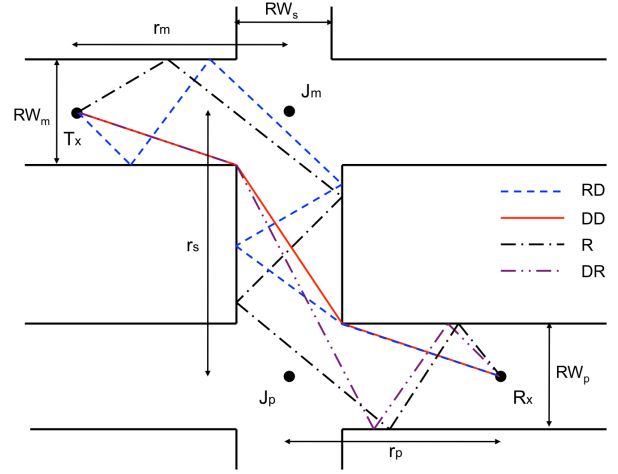


**Figure 5: Graphical example of the geometry in the case NLOS2**

If two vehicles are in an NLOS2 situation then the total path loss is the combination of four main components:  $PL_R$  which is the path loss of all possible rays that reach  $R_x$  only through reflections (black dashed single dotted line in Figure 5);  $PL_{DR}$  which is the path loss relative to all rays that are diffracted on the corner relative to  $J_m$  and then reach  $R_x$  through reflections on the surrounding buildings (purple dashed double dotted line in Figure 5);  $PL_{RD}$  which is the path loss relative to all rays first reflected and then diffracted by the corner relative to  $J_p$  (blue dashed line in Figure 5);  $PL_{DD}$  which is the path loss relative to the rays that diffracted both on the corner relative to  $J_m$  and on the corner relative to  $J_p$  (red solid line in Figure 5). These four components ( $PL_R$ ,  $PL_{DR}$ ,  $PL_{RD}$  and  $PL_{DD}$ ) are functions of the wavelength and of the geometrical properties of the surrounding environment ( $r_m$ ,  $r_s$ ,  $r_p$ ,  $RW_m$ ,  $RW_s$  and  $RW_p$ ). We refer to the original paper [6] for further details on how these components are computed. Finally the total *PL* is then equal to the sum of these four components:

$$PL = 10 \log \left( 10^{\frac{PL_{DD}}{10}} + 10^{\frac{PL_{DR}}{10}} + 10^{\frac{PL_{RD}}{10}} + 10^{\frac{PL_R}{10}} \right) \quad (4)$$

## 2.5 Sample Propagation

The signal propagation modeled by CORNER can be better understood with two practical examples. Let us assume we have a transmitting vehicle  $T_x$  placed at an intersection in an ideal Manhattan grid road topology. We then move a second receiving vehicle  $R_x$  away from  $T_x$  following the motion pattern shown in Figure 6(a). The movement of  $R_x$  will take it from a LOS situation, then to an NLOS1 situation and finally to an NLOS2 situation. In Figure 6(b) we show the received signal power computed using CORNER at a frequency of 2.4GHz. Each turn in the motion pattern, and consequently an additional corner along the signal path, results in a significant drop in the received power. Figure 6(b) also shows the result of the combination of CORNER and additional fading. In particular we superimposed a Rayleigh distributed additional loss to the deterministic component computed by CORNER. As discussed in Section 2.1, CORNER accounts for the obstruction to the signal propagation provided by the surrounding buildings. In order to account for other environmental obstructions and multipath, one should consider and additional fading component, such as Rayleigh or Rice fading [7]. In Figure 6(c) we show the signal attenuation, at a frequency of 2.4GHz, from a source placed in the

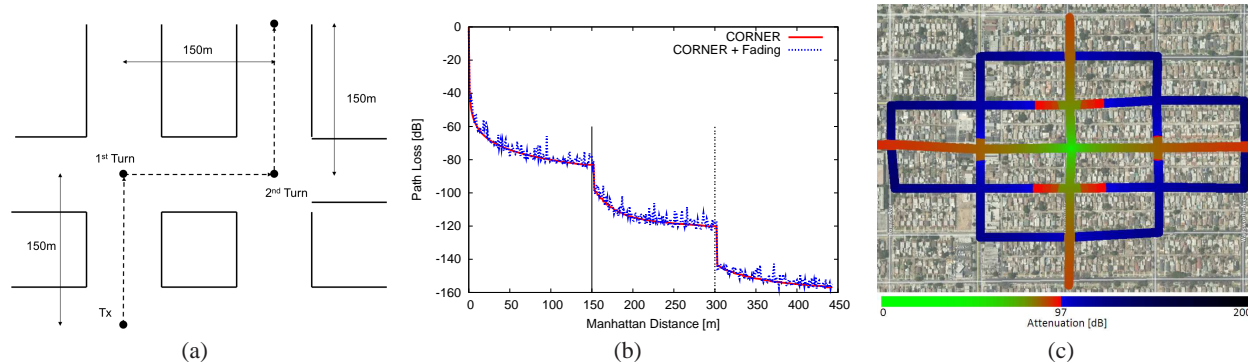


**Figure 6: Urban propagation example from a fixed source ( $T_x$ ) to a mobile destination ( $R_x$ ); (a): road topology and mobility pattern of  $R_x$ ; (b) path loss resulting from the mobility of  $R_x$  using CORNER alone and CORNER with additional Rayleigh fading; (c) example of path loss computation using CORNER for a source placed in the middle of an intersection**

middle of a crossroad. In this case we are using a real road topology extracted from the TIGER database, relative to a residential area in downtown Los Angeles. To highlight the resulting connectivity, we placed a sharp discontinuity in the representation of the attenuation at  $97dB$ , that is the maximum signal attenuation that still grants connectivity for *IEEE802.11b* devices [8]. It is remarkable that, in line of sight, the signal can propagate for several hundred meters. On the contrary the signal sharply degrades behind corners.

### 3. CORNER VALIDATION

The path loss prediction formulae used by CORNER were extensively validated in [6]. However, the authors focused the validation on the accuracy of the predicted received power level. In this section we provide the results our experiment campaign, in which we focused on validating the connectivity resulting from the use of CORNER in a network simulator such as QualNet [9]. In addition, we evaluated the realism of the Link Quality obtained using the channel model implemented in QualNet, providing useful insights for future development of more accurate channel models for urban environment.

Our experiments were carried out using two cars equipped with a laptop with linux OS, a GPS receiver and a IEEE802.11b/g wireless card. The wireless card uses an Atheros chipset allowing the use of the open source driver MadWiFi [10]. To better understand the characteristics of connectivity we performed all the tests placing our application directly on top of the MAC layer. This is possible in Linux using the Ethernet raw sockets package. In other words our application sends and receives packets directly to and from the wireless card buffer, avoiding the use of IP and higher layer protocols that can cause connection delays. We performed two sets of experiments: one to assess the connectivity around corners, involving fixed and mobile nodes; a second set to assess the link quality around corners using fixed locations. We performed all of our experiments in a Los Angeles residential area<sup>1</sup>. We then reproduced the same scenarios using the implementation of CORNER for QualNet [9] network simulator, and compared the obtained results with the ones obtained in reality. It is important to point out that the real experiments are affected by environmental interference that can not be easily reproduced in simulation. In fact, we were able to detect 227 distinct Access Points (APs) in the area. Figure 7 shows the channel occupancy of all the detected APs. Our experiments were performed using the automatic channel detection. With

<sup>1</sup>Lat: 34.053397N, Lon: 118.442660W

this setting the wireless card scans all the band and chooses the least interfered channel to operate on. Although this setting guarantees the lowest possible level of interference, the high number of surrounding APs will affect heavily the packet reception, especially in the case of broadcast for which the RTS/CTS/DATA/ACK procedure is not used and retransmissions are not allowed. In order to reproduce this kind of interference, we would need information that is not possible to gather, such as the location of access points and the kind of data traffic that is running on them. In addition, as illustrated in Figure 7, not only the orthogonal channels 1, 6 and 11 are occupied by surrounding APs. The use of non-orthogonal channels seriously affects the carrier sensing procedure, causing a high rate of transmission failures.

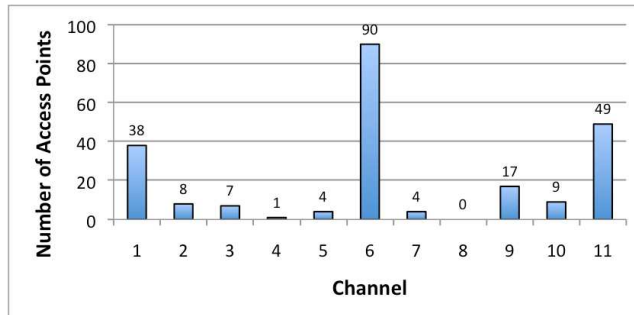


**Figure 7: Environmental Interference: Channel occupancy of APs in the area**

#### 3.1 Connectivity Experiments

To assess the connectivity around corners we performed both Fixed-to-Mobile and Mobile-to-Mobile experiments. In both setups the nodes are periodically broadcasting a packet containing their geographic coordinates and the GPS timestamp. The frequency of transmission has been set to 10 packets per second.

*Fixed-to-Mobile.* We performed two different tests with one car revolving around a block and the other fixed, first in the middle of the block and then placed at an intersection. In both experiments the fixed car periodically sends out broadcast packets. The mobile car then saves the geographic coordinates where it received each packet. Figures 8 and 9 show, plotted on Google Earth [11], the set of locations where packets were received both for the field test



Figure 8: Fixed-to-Mobile experiment: comparison between field experiment (blue squares) and simulation (yellow triangles). Representation of the locations in which the moving car received a packet generate from a source placed in the middle of the road block.



Figure 9: Fixed-to-Mobile experiment: comparison between field experiment (blue squares) and simulation (yellow triangles). Representation of the locations in which the moving car received a packet generate from a source placed at the intersection.

(blue squares) and in simulation (yellow triangles). It is remarkable that the simulated connectivity is very similar to the real one. In addition we can see that in simulation the number of received packets is much higher. This is a consequence of the surrounding environmental interference that cannot be reproduced in simulation, as discussed previously.

*Mobile-to-Mobile.* To further validate the propagation model we also ran a Mobile-to-Mobile experiment. The two involved cars were revolving around the block in opposite directions. One of the cars would store the position it received the packet at, together with the position of the other car included inside the packet. Figure 10 shows the comparison of the real experiment and the simulation. Each single received packet is represented as a red line joining the receiving and sending positions represented with blue squares. We can observe that the model well reflects the reality avoiding the transmission of packets that traverse the block.

### 3.2 Link Quality

To validate Link Quality simulation results, we performed two testbed experiments involving propagation around a corner.

- Experiment A: We fixed a *sender* node (S) at on ent of a road and we moved the receiver to five different positions,

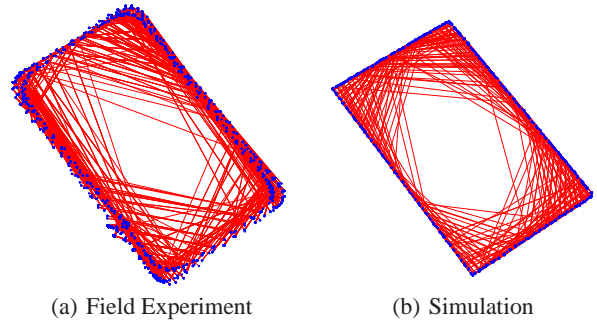


Figure 10: Mobile-to-Mobile experiment: connectivity comparison between field experiment and simulation. Each link (red solid lines) represents a successfully transmission between two locations (blue dots).

first in Line of Sight (positions 1 through 4) and then around a corner (positions 1 and 2), as shown in Figure 11(a).

- Experiment B: We fixed a *sender* node (S) next to an intersection and we moved the receiver to six different positions, first in Line of Sight (position 1) and then around a corner (positions 2 through 4), as shown in Figure 11(c).

In both experiments, for each position of the receiver, the *sender* sent 500 unicast packets. The use of unicast packets minimizes the impact of surrounding interference, that is not negligible. We defined the Link Quality as the number of packets received divided by the number of packets sent. We present the comparison between the Link Quality obtained in the field experiments and the Link Quality obtained with the QualNet simulator, combining CORNER with additional fading. In Figures 11(b) and 11(d), for experiments A and B respectively, we compare the Link Quality obtained in the field experiments and the Link Quality obtained using Rice and Rayleigh fading [7]. As expected, the Rician fading can reproduce well the Link Quality for the LOS situations, namely positions 1 through 4 in experiment A and position 1 in experiment B. However, the Rice model performs poorly in the remaining NLOS situations. In these cases, the Rayleigh fading is better, as expected. In conclusion, to better reproduce the Link Quality in simulation, the channel model should be modified to use the appropriate fading model in LOS and NLOS situations, exploiting the classification provided by CORNER.

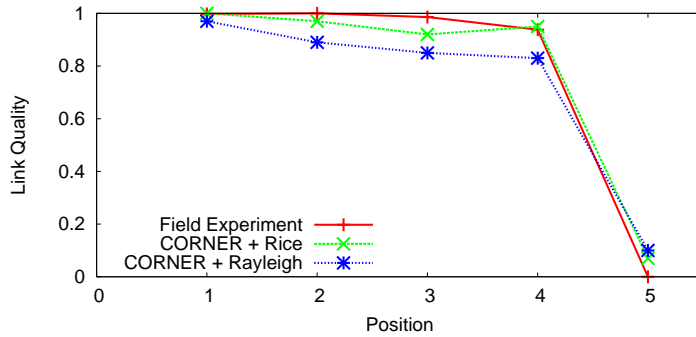
## 4. IMPACT ON VANET SIMULATIONS

Due to the high cost of real vehicular testbeds, simulation is still the only means to assess performance of large scale vehicular networks. It is then crucial that the models used in simulation reflect reality as much as possible. However most of the research performed on VANETs assumes a *flat* propagation model, such as Two Ray. Some simulation studies use a reduced radio range, in the attempt to avoid connections that would traverse city blocks. These solutions may produce very misleading results. In this section, we assess the main drawbacks of using a *flat* propagation model. For this purpose we generated a mobility pattern using the VERGILIUS Urban Traffic Scenario Generator [12]. We used a map of size 500 by 500 meters located in Los Angeles downtown<sup>2</sup>, with a total entering flow of 5000 vehicles per hour, uniformly distributed over the entry points. We fed the resulting traffic pattern

<sup>2</sup>Centered at Lat: 34.044000N, Lon: 118.434100W



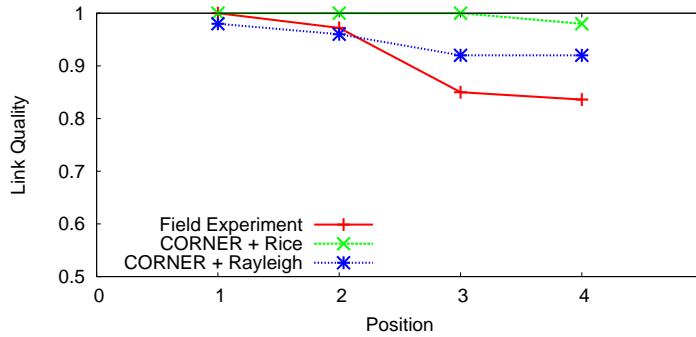
(a) Experiment Setup A



(b) Experiment A: Link Quality for fixed receiver positioned at increasing distance



(c) Experiment Setup B



(d) Experiment B: Link Quality for fixed receiver positioned at increasing distance

**Figure 11: Link Quality evaluation experiment: comparison between field experiment and CORNER combined with Rayleigh and Rician fading for two experimental setups.**

to CORSIM [13] obtaining a mobility trace lasting 300s. In order to evaluate the major differences between CORNER and a *flat* propagation we used the VERGILIUS Trace Analyzer that extracts relevant network metrics from mobility traces. In the following we provide a brief description of each metric, we refer to the original VERGILIUS paper [12] for further details:

- **Connectivity Index:** is defined in the interval  $[0, 1]$ . It is a measure of how well the network is connected, for example, a value of 1 represents a fully connected network at all times.
- **Average Hop:** represent the average “distance” in terms of hop count among all nodes in the network, averaged over time.
- **Node Degree:** represents the size of the neighborhood of each node, averaged over all nodes and over time.
- **Link Duration:** is the time interval in which two nodes are connected to each other, averaged over all nodes and over time.

We computed the aforementioned metrics for three different propagation schemes:

- **CORNER:** Nodes use a transmitted power of  $8.5dBm$  and a receiver sensitivity of  $-89dBm$ .
- **R250:** We used the Two Ray model with a transmitted power of  $8.5dBm$  and a receiver sensitivity of  $-89dBm$  that leads to a propagation range of 250 m. This is the most common propagation model used in simulation studies.

- **R80:** We used the Two Ray model with a reduced transmitted power of  $-2.5dBm$  and a receiver sensitivity of  $-89dBm$  that leads to a propagation range of 80 m. This is one of the most common solution adopted to avoid connections across buildings.

In Figure 12, we show a snapshot of the network connectivity for each of the considered propagation schemes. In particular, Figure 12(a) shows the connectivity graph computed using CORNER. In Figure 12(b) we show the connectivity graph for the same scenario using a simple geometric range of 80 meters (R80), finally 12(c) shows the connectivity graph for a geometric range of 250 meters (R250). It is evident that both *flat* propagation schemes have highly impacting drawbacks. In particular R250 is too optimistic and allows connections that traverse one or more city blocks. Conversely R80 is too pessimistic, as it does not allow connection traversing city blocks but at the same time removes connections between nodes that are in line of sight and therefore should be able to communicate, thus creating unrealistic network partitions. We can observe these drawbacks impacting the connectivity metrics of the network. In Table 1 we report the results of our analysis. For both CORNER and R250 the network is almost fully connected. Instead for R80 the network is often partitioned, indeed each node, on average, can reach only 69% of the network. For the *flat* propagation schemes the Number of Hops merely depends on the geometrical size of the network. For CORNER instead this is related to the surrounding environment. Indeed the area considered includes a 4 by 2 blocks city portion that justifies the average of 2.3 hops. The lower connectivity for R80 results in a much lower Node Degree with respect to R250. For CORNER the Node Degree is lower than

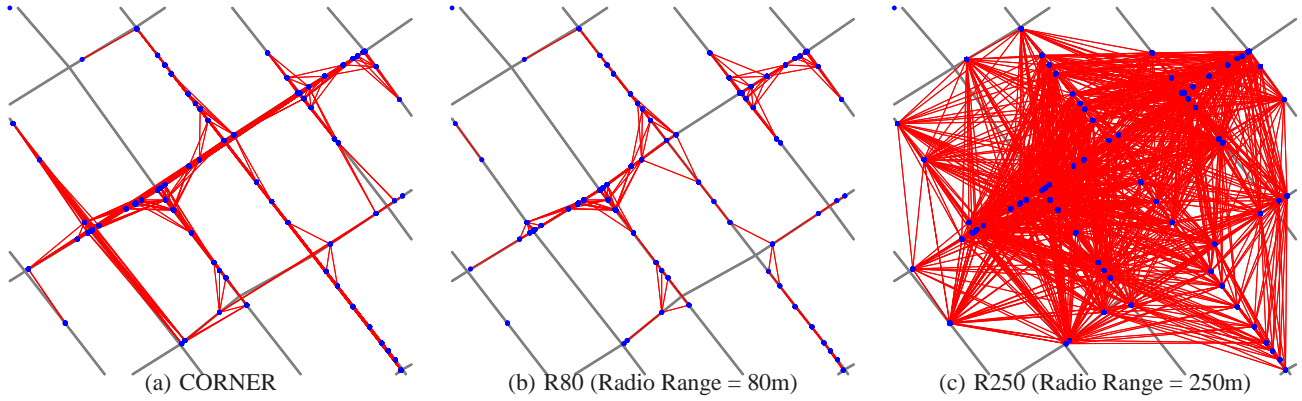


**Figure 12: Connectivity graphs for 95 nodes in the 500 by 500 meters area in Los Angeles, California:** (a) shows the connectivity graph using CORNER, (b) shows the connectivity graph using a geometric range of 80m and (c) shows the connectivity graph using a geometric range of 250m.

R250 due to all nodes that are behind corners and cannot connect to each other, but higher than R80 as the nodes that are in line of sight can still communicate. For the *flat* propagation schemes the Link Duration is related to the ratio between the radio range and the relative speed of nodes. Indeed we can observe an almost linear relationship between R80 and R250. This is not true for CORNER. In fact, the link Duration does not depend only on the relative speed but also on the surrounding environment.

Metric	CORNER	Range 250m	Range 80m
Connectivity Index	0.99	0.99	0.69
Average Hops	2.3	1.5	4.2
Average Node Degree	19.9	47.2	7.6
Average Link Duration	16.2	24.52	11.6

**Table 1: Trace analysis for the different propagation schemes**

We then simulated the resulting network using the QualNet simulator using IEEE802.11b with fixed data rate of 2Mbps, AODV as routing protocol and an increasing number of Constant Bit Rate (CBR) flows. The sources and destinations of the CBR flows are chosen randomly. The flows consist of 512 bytes packets generated 8 times per second for a resulting flow of 32 Kbps. The duration of the CBR connection is random with an average of 20s. In Figure 13 we show the Delivery Ratio as a function of the percentage of nodes initiating a CBR connection comparing the three propagation schemes. As it is illustrated in Figure 13, a *flat* propagation scheme can produce very misleading results. In the case of R250 such a wide range causes all the nodes to compete for the channel even though they are far apart from each other. This causes a severe drop of the delivery ratio for high load of the network. In the CORNER case instead, the severe drop occurs for much lower network load. This is due to the concentration of the load onto nodes that are at intersections. In fact these nodes are the only ones that are able to route traffic through different parts of the network. Once these nodes are overloaded the performances drop drastically. For R80 we can observe that the Delivery Ratio is consistent with the total connectivity for low network load. However, for high load, the performances are slightly better as the local traffic is affected by less interference and less channel contention resulting in a better delivery ratio.

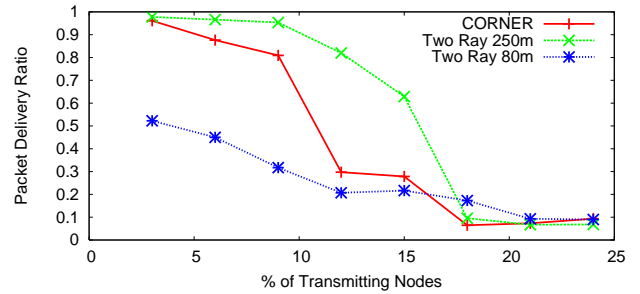


**Figure 13: Comparison of Delivery Ratio over the same scenario using different propagation models**

## 5. RELATED WORK

In the last few years, most of the proposed protocols and applications for VANET have been evaluated through simulation studies. The modeling of urban mobility has improved substantially and reached a very good level of realism. However the accurate representation of mobility is voided by the use of unrealistic statistical *flat* propagation models. In [14] Kotz et al. present a survey on the most commonly used propagation schemes in VANET simulation studies. The most popular propagation model is Two Ray [7] that is very easy to implement and provides a path loss prediction based solely on the geometric distance between two nodes. As Two Ray does not take into account any obstruction along the signal path, it is usually combined with a Log-normally distributed additional shadowing component [15]. This shadowing component simulates the movement of vehicles around large objects such as buildings. However, using this approach, obstructions are represented statistically, and therefore could be placed between vehicles that are actually in Line of Sight or, vice versa, not present between vehicles that are not in Line of Sight. This results in a complete dissociation between the path loss and the mobility of the nodes, invalidating the realism of the mobility.

In order to preserve the verisimilitude of the mobility the path loss prediction must be correlated to the environment the vehicles are moving in, using a propagation model specific for urban scenarios and that deterministically takes into account obstructions along the signal path. Numerous propagation models for urban environment have been proposed so far. However, most of them are specific

for cellular networks and model the propagation between base stations and mobile nodes. Indeed the use of ad hoc networks in urban environment is a new topic of research, thus the mobile to mobile channel still needs to be modeled in detail. The best approach is then to adapt existing cellular network propagation models to V2V communications. A first attempt in this direction has been proposed in [16] that presents the details of the implementation of the propagation model presented in [17] for the simulator ONNeT++ [18]. The chosen propagation model uses different formulae for the Line of Sight (LOS) and non Line of Sight (NLOS) cases. However, to distinguish between these two cases, the simulator uses information obtained from the mobility simulator, without performing any reverse geocoding. This makes both the implementation and the model very simulator and mobility model dependent. Indeed, this implementation works only with the Manhattan Grid Mobility Model implemented in OMNet++ and cannot be ported to any other simulator. In addition the authors do not provide any validation of resulting connectivity. Another similar technique has been proposed in [19]. In this paper the authors assess the performance of several routing protocols for VANET, under realistic propagation conditions. The propagation model used is the one presented in WINNER project [20]. The main drawback of this model is the assumption that the transmitter antenna is placed on top of a building, at least 5 meters above the ground. Therefore in case of NLOS, the signal traverses a vertical path that involves a corner created by the roof of the building closer to the mobile node. In [19], this assumption has been loosened and the signal is assumed to traverse a horizontal path involving a corner created by the intersection between the mobile nodes. This adaptation however might introduce inaccuracies, that are not possible to quantify as the authors do not provide any validation. In addition, no detail is provided on how the model distinguishes between LOS and NLOS situations.

## 6. CONCLUSIONS

We presented CORNER, a lightweight yet accurate propagation model for urban scenarios. CORNER features a simulator-independent path loss computation that deterministically accounts for environment obstructions, providing a good correlation between mobility and propagation. CORNER uses a specific reverse geocoding technique aimed to identify the path followed by the radio signal. Each pair of vehicles is classified into three possible cases: Line of Sight, Non Line of Sight with one corner along the signal path and Non Line of Sight with two corners along the signal path; once the scenario has been identified, CORNER implements the path loss prediction formulae presented in [6]. Nevertheless the classification is independent from the formulae to apply and therefore more accurate or more specific formulae could be easily implemented. Experiments performed on the road show that CORNER accurately predicts the network connectivity. Insights from our Link Quality evaluation suggest that a channel model aware of the propagation situation would provide a better representation of reality. Finally, we presented the most impacting inherent defects that characterize all simulation studies performed using *flat* propagation models.

## Acknowledgment

Eugenio Giordano would like to thank Microsoft Research for financially supporting this work through its PhD Scholarship Programme.

Raphael Frank would like to thank the National Research Fund of Luxembourg (FNR) for financially supporting this work.

We are grateful to our shepherd Onur Altintas, for his valuable

advises in improving the presentation of this work and to the anonymous reviewers for their thoughtful comments.

## 7. REFERENCES

- [1] IEEE 802.11 working group. IEEE P802.11pTM/D3.0 Draft Standard for Information Technology - Amendment 7: Wireless Access in Vehicular Environments. ANSI/IEEE Std 802.11, 1999 Edition (R2007).
- [2] Michel Ferreira, Hugo Conceição, Ricardo Fernandes, and Ozan Tonguz. Stereoscopic aerial photography: An alternative to model-based urban mobility approach. In *Sixth ACM International Workshop on Vehicular Inter-NETworking (VANET)*, September 2009.
- [3] Antony Rowstron and Giovanni Pau. Characteristics of a vehicular network. Technical Report 09-0017, University of California Los Angeles, Computer Science Department, July 2009.
- [4] Stephan Bohacek, Vinay Sridhara, Gaurav Singh, and Andjela Ilic. The udel models - manet mobility and path loss in an urban/suburban environment. Technical report, University of Delaware, Electrical Engineering Department, 2004.
- [5] V. Sridhara and S. Bohacek. Realistic propagation simulation of urban mesh networks. *Computer Networks*, 51(12):3392–3412, 2007.
- [6] Q. Sun, S. Y. Tan, and Kah C. Teh. Analytical formulae for path loss prediction in urban street grid microcellular environments. *IEEE Transactions on Vehicular Technology*, 54(4):1251–1258, July 2005.
- [7] T.S. Rappaport. *Wireless communications*. Prentice Hall PTR Upper Saddle River, NJ, 2002.
- [8] IEEE 802.11 working group. IEEE 802.11, part 11: Wireless LAN medium access control (MAC) and physical layer (PHY) specifications. ANSI/IEEE Std 802.11, 1999 Edition (R2007).
- [9] Scalable-Networks. QualNet Network Simulator. <http://www.scalable-networks.com>, Last Accessed in April 2010.
- [10] MadWiFi Project. <http://madwifi-project.org/>, Last Accessed in April 2010.
- [11] Google Inc. Google Earth. <http://earth.google.com/>, Last Accessed in April 2010.
- [12] Eugenio Giordano, Enzo De Sena, Giovanni Pau, and Mario Gerla. Vergilius: A scenario generator for vanet. In *2010 IEEE 71st Vehicular Technology Conference: VTC2010-Spring*, 2010.
- [13] University of Florida. Traffic Software Integrated System - Corridor Simulation. <http://mctrans.ce.ufl.edu/featured/tsis/>, Last Accessed in April 2010.
- [14] D. Kotz, C. Newport, R.S. Gray, J. Liu, Y. Yuan, and C. Elliott. Experimental evaluation of wireless simulation assumptions. In *Proceedings of the 7th ACM international symposium on Modeling, analysis and simulation of wireless and mobile systems*, pages 78–82. ACM, 2004.
- [15] W. C. Y. Lee. *Mobile Communications Engineering*. McGraw-Hill, 1982.
- [16] R. Nagel and S. Eichler. Efficient and realistic mobility and channel modeling for VANET scenarios using OMNeT++ and INET-framework. In *Proceedings of the 1st international*

- conference on Simulation tools and techniques for communications, networks and systems & workshops*, page 89. ICST (Institute for Computer Sciences, Social-Informatics and Telecommunications Engineering), 2008.
- [17] STS Chia and P. Snow. Characterising radio-wave propagation behaviour at 1700 MHz for urban and highway microcells. In *IEE Colloquium on Micro-Cellular Propagation Modelling*, page 11, 1992.
- [18] OMNet++. <http://www.omnetpp.org/>, Last Accessed in April 2010.
- [19] R. Bauza, J. Gozalvez, and M. Sepulcre. Operation and Performance of Vehicular Ad-Hoc Routing Protocols in Realistic Environments. In *IEEE 68th Vehicular Technology Conference, 2008. VTC 2008-Fall*, pages 1–5, 2008.
- [20] Wireless World Initiative New Radio (WINNER) Information Society Technology. D1.1.1. WINNER II interim channel models. <http://www.ist-winner.org/deliverables.html>, Last Accessed in April 2010.